Available online at www.CivileJournal.org

# Civil Engineering Journal

(E-ISSN: 2476-3055; ISSN: 2676-6957)

Vol. 10, No. 12, December, 2024

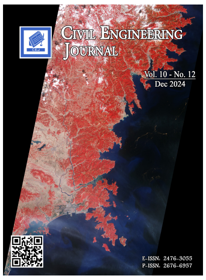


# The Performance of Geosynthetic Reinforcement Road Pavement Over Expansive Soil Subgrade

Hairulla [1*], Tri Harianto [1], Abdul Rahman Djamaluddin [1], Ardy Arsyad [1]

[1] *Department of Civil Engineering, Hasanuddin University, Makassar, 92171, Indonesia.*

Received 31 July 2024; Revised 15 November 2024; Accepted 23 November 2024; Published 01 December 2024

**Abstract**

One of the problems faced in infrastructure development, especially roads, is problematic soils, including expansive soils, which are distributed around 20% of national road construction in Indonesia. Geosynthetics are reinforcement materials that can be used to overcome problematic soils. The study aimed to determine the behavior of expansive soil with geosynthetic reinforcement against swelling potential and swelling pressure in the wetting cycle. The research utilized an experimental approach involving three test concepts. The first was a control test without reinforcement. The second included a combination of geogrid, geotextile, and geomembrane layers, while the third utilized an H2Rx reinforcement layer. Analysis was carried out on the development potential and pressure; the test was carried out for 57 days using displacement sensors and pressure sensors, and data recording was carried out every 5 seconds using a computer. The findings from the results of this study indicated that the presence of reinforcement using a geosynthetic reinforcement layer can overcome the behavior that occurs in expansive soils with swelling potential and swelling pressure. The novelty of this research is the inclusion of a geosynthetic reinforcement layer on expansive soil combined with a drainage layer in the pavement subgrade.

*Keywords:* Geosynthetics; Expansive Soil; Swelling Potential; Swelling Pressure.

## 1. Introduction

In infrastructure development, soil is crucial as it supports structural placement. Therefore, to ensure stability, soil must have adequate bearing capacity. Soil is a construction material readily available in the field; thus, soil with good characteristics can be used as a construction material, significantly impacting the economic value of the project [1]. Indonesia has diverse soil characteristics with varying bearing capacities. In the context of rapidly growing infrastructure development, particularly road construction at the district, provincial, and national levels, it is often unavoidable that certain sites with poor soil conditions are unable to support construction due to insufficient bearing capacity. Wetlands are areas where the soil is saturated with water. These wetlands include swamps, brackish, and peat. Approximately 20 million hectares, or 10% of Indonesia's land area, consist of expansive soils, primarily composed of soft clay and peat. The distribution of expansive soils in Indonesia is along the north coast of Java, the east coast of Sumatra, the west, south, and east coasts of Kalimantan, the south coast of Sulawesi, and the west and south coasts of Papua. Expansive soils have low pH levels, high cation exchange capacity, low base saturation, and low K, Ca, Mg, P, and microelements (such as Cu, Zn, Mn, and B).

Engineering intervention is essential, particularly for subgrade, to prevent structural failure due to insufficient bearing capacity. In this case, reinforcement using geosynthetics is implemented to improve the strength of expansive

* Corresponding author: hairulla21d@student.unhas.ac.id

http://dx.doi.org/10.28991/CEJ-2024-010-12-020

soil and to control its shrinkage and swelling behavior. For subgrade soils with expansive characteristics, moisture content changes significantly affect soil swelling movements that can affect the pavement above. Different swellings of the subgrade will damage the pavement and interfere with traffic comfort. For this reason, it is necessary to handle subgrade soils that have expansive properties such as the structure of the Moisture Barrier layer (Barrier), the separation filtration layer, the Drenage layer (Drenage), and the Stiffening Reinforcement layer. In this research, a testing scheme of pavement subgrade reinforcement with geosynthetic materials was carried out by comparing Geogrid, Geotextile, and Geomembrane reinforcement materials as reinforcement layers, barrier layers, and impermeable layers for the first scheme model. For the second scheme model, they link using H2Rx functions simultaneously as a reinforcement layer, barrier, and drainage layer. The theoretical foundation and references for this research are based on previous studies. Geosynthetics such as H2Rx, Geogrid, Geotextile, and Geomembrane were selected for reinforcing the pavement layer due to their proven effectiveness, which is the primary reason for choosing these materials.

Large-scale pullout tests were conducted using geogrid specimens covered with soil. On the other hand, bone pullout tests were performed using longitudinal and transverse reinforcement. For the use of geogrids in this investigation, the nature of the mechanism significantly affects the interfacial shear strength along the longitudinal direction [2]. Based on the results of infiltration tests on geosynthetics and sand in layers and drainage, using geosynthetics as layers and drainage in saturated soil had the same behavior as conventional layers and sand [3]. Fiber reinforcement is a good alternative in projects involving local soil improvement and reinforcement of thin soil layers, such as geotextiles and geogrids [4]. Although this decrease in strength was initially caused along the fiber-soil interface, the results from this test suggest that the effect of fibers on pore pressure during CU testing may provide higher adequate strength [5]. Geosynthetics function as reflective crack treatment in asphalt layers, separation, road base stabilization, soft subgrade stabilization, and horizontal drainage [6]. In addition, reinforcement performed to mitigate longitudinal cracking in a pavement constructed on a highly plastic expansive clay subgrade showed that the performance of geogrids can prevent the increase of longitudinal cracking in the pavement section compared to those without geogrids showing significant cracking [7]. Shear strength behavior using Geogrid is higher than Geotextile for layers and interfaces [8]. All test methods, field, laboratory, and numerical study results show geosynthetics are very influential on the performance of the pavement; further research needs to be done to get a better empirical design approach [9]. The geogrid will resist tensile stresses in the pavement layer when receiving vehicle loads. This mechanism will reduce pavement flexure. As a result, the road service time increases with the same traffic load [10].

Previous studies have found that soil reinforcement using geosynthetics can significantly improve the bearing capacity of soils. The lateral swelling pressure of expansive soils, which was included in the total lateral pressure, often results in instability and even shear failure of retaining walls [11]. Geotextile is used as reinforcement to increase the bearing capacity, where the Geotextile functions as a material to distribute the load to the soft soil. When the embankment height is less than 10 m, geogrids have the advantage of reducing stress and deformation [12]. A comprehensive understanding of the behavior of expansive soils requires an explanation of the phenomenon of clay particle surface and soil microstructure changes [13]. Laboratory tests were conducted to obtain Nanning natural expansive soil's saturated undrained shear strength by considering the combined effects of development with load and wet-dry cycling [14]. Soil swelling that causes lateral and axial stresses can threaten the safety and stability of geotechnical structures [15]. Geogrids are placed in the ground, where the geogrid serves to control the swelling of the soil volume [16]. Highly plastic clays experience a cycle of expansion and contraction during the wet and dry seasons, which usually makes the soil soft and can cause failure in the wet season [17]. Monitoring results show soil bags' effectiveness in preventing moisture migration, reducing swelling potential, and improving slope stability [18]. Earthbags can be considered a semi-permeable material as they exhibit good drying characteristics [19]. Field and laboratory investigations examined the nature of microscopic deformation, material properties, structural properties, and slope stability [20]. The wetting and drying process is simulated by soaking the test specimen with water and then removing the water from the test box to dry the specimen [21]. The local deformation of geosynthetics, such as geogrids and nonwoven and woven geotextiles, is measured to analyze the stability of geosynthetic-reinforced soil structures. [22].

Based on previous research that used geosynthetic materials for expansive soil reinforcement, the main distinction in this study is the comparison between the reinforcement of Geogrid, Geotextile, and Geomembrane layers, as well as the H2Rx layer. The Geogrid, Geotextile, and Geomembrane layers have different functions. They were used as a unity for the expansive soil reinforcement layer compared to H2Rx, which functions as a reinforcement layer, barrier, and drainage layer. In this research, the reinforcement of expansive soil was carried out using geosynthetic materials, namely geogrid, geotextile, and geomembrane, as well as H2Rx (Hybrid Layer) on a laboratory scale. This study tested three models: without reinforcement treatment, reinforcement with geogrid, geotextile, and geomembrane; and reinforcement with H2Rx (hybrid layer). For the testing process, all test samples were given water to observe the swelling process until constant swelling or no more swelling occurred with either the first, second, or third testing schemes. In the data collection process, deformation measurements were taken on three models using displacement and ground pressure sensors [23].

## 2. Materials and Methods

### 2.1. Materials

The materials used in this study were expansive clay used as a layer and subgrade, which is the object of research; geosynthetics, including geogrid as a reinforcement material (stiffening reinforcement); Geotextile as a separation and filtration material; geomembrane as a barrier material; and coarse aggregate that had permeable properties (drainage). Granular soil that had a class B specification for subbase and foundation layer materials. The materials used in this study can be seen in Figure 1.

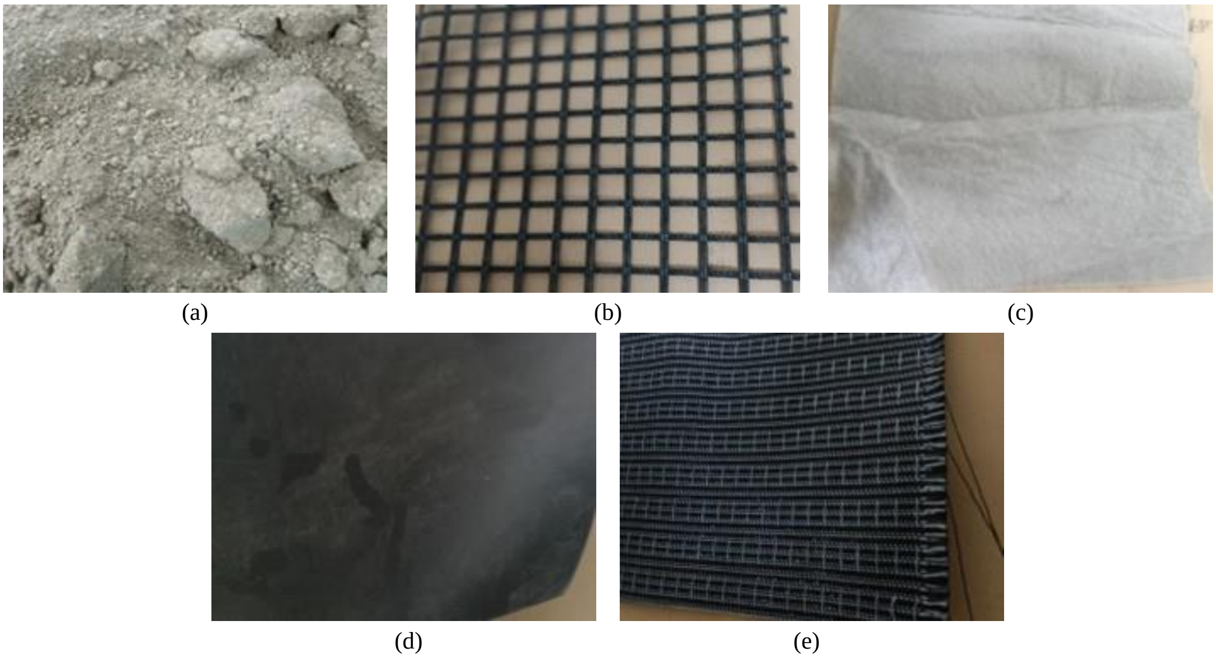


**Figure 1. Testing Sample, (a) Expansive soil, (b) Geogrid, (c) Geotextile, (d) Geomembrane, (e) H2rX**

#### 2.1.1. Characteristics of Geosynthetics

This study used four types of geosynthetics: geogrid, geotextile, geomembrane, and H2rX, which can be seen in Table 1 for their characteristic values. The distinctive properties of the geogrid material used were biaxial, which had a tensile strength of 80 kN/mm; Geotextile nonwoven material, which had a tensile strength of 9.5 kN/m; geomembrane, which had a tensile strength of 11.6 kN/mm, and for H2Rx material, the tensile strength was 20 kN/mm. The materials used in this research as reinforcement materials were manufactured materials resistant to environmental conditions in terms of durability, biodegradability, or potential effects on the surrounding soil.

**Table 1. Characteristics of Geosynthetics**

| Geogrid | | Geotextile nonwoven | | Geomembrane | | H2RX | |
|---|---|---|---|---|---|---|---|
| Tensile Strength (md and cd) | 80 & 80 kN/m | Tensile Strength | 9.5 kN/m | Thickness | 0.75 mm | Tensile Strength 2% & 5% | 20 & 50 kN/m |
| Tensile Strength at 5% Strain | 44 kN/m | Tensile Elongation | 75/35 | Tensile Properties Yield & Break | 11.6 & 21 kN/m | CBR Puncture | 9 kN |
| Tensile Elongation (Strain Initial Strength) | 8% | CBR Puncture | 1500 N | Resin density | > 0.932g/cc | Pore Size | 0.30 mm |
| | | Apparent Opening Size | 0.26 mm | | | Permeability | 1500 l/m²/min |
| | | Nominal Mass | 125 g/m$^2$ | | | Moisture movement, vertical and horizontal | 150 & 1900 mm |

#### 2.1.2. Characteristics of Expansive Soil

From the results of expansive soil testing, characteristics were obtained, physical properties that fall into the expansive soil category are presented in Table 2, and values for mechanical properties. The results of the physical properties test, namely the sieve analysis test [24, 25], showed that the test material was more dominant in refined grains, accounting for as much as 65% or greater than 50% of the fine-grained soil content, with silt soil grain content of 22% and clay grain content of 43%, which was included in the fine-grained soil category, where this result was one of the requirements for entering the expansive soil category. Based on the test results obtained for the liquid limit (LL) test [26] by 130%, the plastic limit (PL) test [26] by 62%, the plastic index (PI) test [26] results by 69%, and the shrinkage limit (SL) test results [27] by 12%. Based on the results of the Atterberg limits test, it showed that the soil used in this test was expansive. This was also supported by the free swelling index test, whose value was 132.14%. For soil calcification results based on AASHTO [28] and USCS [29], the test samples were also categorized as soils with a high plasticity index relative to the liquid limit and can undergo very high-volume changes. The soil characteristics test results categorized the soil used as expansive soil.

For testing, the mechanical properties of the samples used from the test results can be explained as follows: the results of the compaction test using the standard compaction method. ASTM D698-12 [30] Obtained the maximum dry weight ($\gamma d$) of 1.31 gram/cm³ and the optimum water content of 35.5%. For the California Bearing Ratio (CBR) test results [31] Unsoaked testing was 13.5%, and soaked testing was 1.20%. The testing results showed a swelling potential of 76.1% and a swelling pressure of 294.2 kPa. The results of testing the mechanical properties of soil materials used in both California Bearing Ratio (CBR) tests showed that the effect of soaking the soil samples tested had a significant impact on the bearing capacity of the soil used in this study, which can be seen from the results of the California Bearing Ratio (CBR) test, unsoaked conditions, and soaked conditions. Likewise, the results of the potential swelling test and the swelling pressure show that the test results obtained a huge pore volume change, which resulted in the soil losing a huge bearing capacity, as can also be seen from the California Bearing Ratio (CBR) test results between the unsoaked test results and the soaked testing. From the swelling pressure test results, the pressure caused to the test sample during the wetting process increased significantly. This shows that the test results of swelling potential and swelling pressure are directly proportional, where the volume changes caused by swelling potential result in swelling pressure.

**Table 2. Soil Characteristics**

| Testing | Testing Results | Unit | Testing Standards |
|---|---|---|---|
| ***Physical Properties Testing*** | | | |
| Water content (%) | 2.72 | % | ASTM D-2216-98 [32] |
| Specific Gravity (*GS*) | 2.62 | | ASTM 0854-14 [33] |
| ***Sieve Analysis*** | | | |
| a. *Gravel* | 0 | % | ASTM D7928–17 [25] and ASTM C117–13 [24] |
| b. *Sand* | 35 | % | |
| c. *Silt* | 22 | % | |
| d. *Clay* | 43 | % | |
| ***Atterberg Limits*** | | | |
| a. Liquid Limits (*LL*) | 130 | % | ASTM D4318–10 [26] |
| b. Plastic Limit (*PL*) | 62 | % | ASTM D4318–10 [26] |
| c. Plastic Index (*PI*) | 69 | % | ASTM D4318–10 [26] |
| d. Shrinkage Limit (*SL*) | 12 | % | ASTM D4943–08 [27] |
| ***Soil Classification*** | | | |
| Clasification AASHTO | A-7-6 | | AASHTO M 145-91 [28] |
| Clasification USCS | CH | | ASTM D 2487–17 [29] |
| Free Swell index testing (%) | 132.14 | % | |
| ***Mechanical Properties Testing*** | | | |
| ***Compaction*** | | | ASTM D698-12 [30] |
| a. Maximum Density (gr/cm$^3$) | 1.31 | Gram/Cm$^3$ | |
| b. Optimum Water Content (%) | 35.5 | % | |
| ***CBR*** | | | ASTM D-1883 [31] |
| **CBR Design Unsoaked (%)** | | | |
| Density 90 % | 13.5 | % | |
| **CBR Design Soaked (%)** | | | |
| Density 90 % | 1.2 | % | |
| Swelling Potential Density 90% | 76.1 | % | |
| Swelling Pressure Density 90% | 294.2 | kPa | |

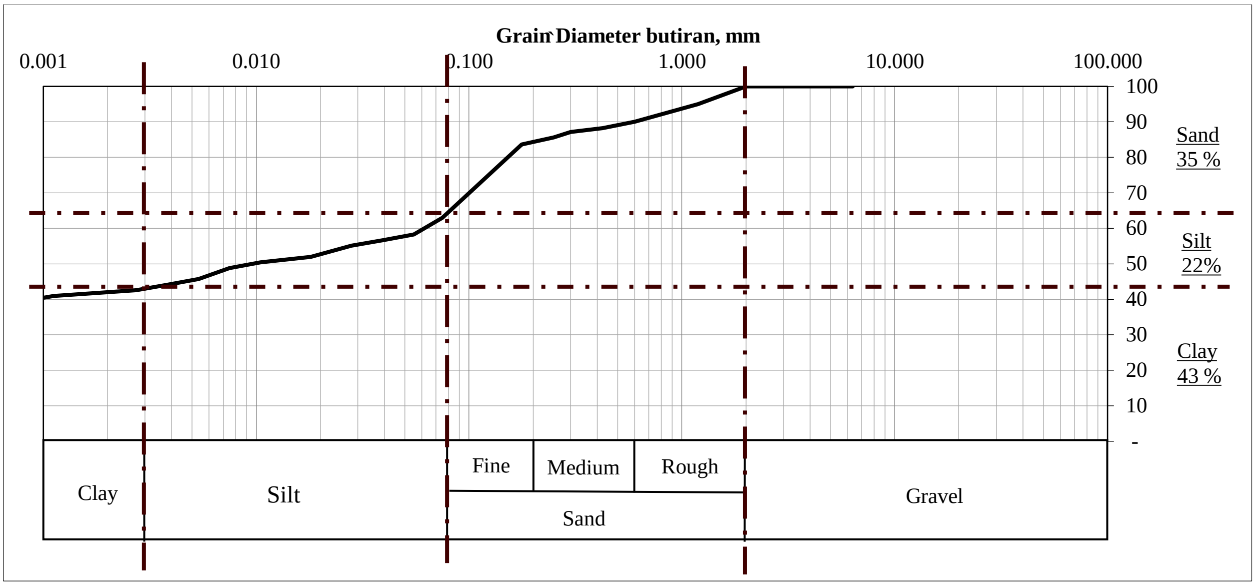


**Figure 2. Distribution Granulation Diagram Material Soil**

## 2.2. Research Methods

The research method used was quantitative, with an experimental database in the laboratory. This research was designed by referring to previous research, a source of development, and correlated and relevant novelties. This research also referred to ASTM testing standards, such as physical properties, referring to the testing standards in the reference, and for testing mechanical properties, referring to ASTM standards, which refer to testing standards. The research implementation procedures were carried out systematically and comprehensively so that each experimental result or analysis obtained from testing could be collaborated. The detailed research procedure for road layer and foundation model tests is shown in Figure 3.

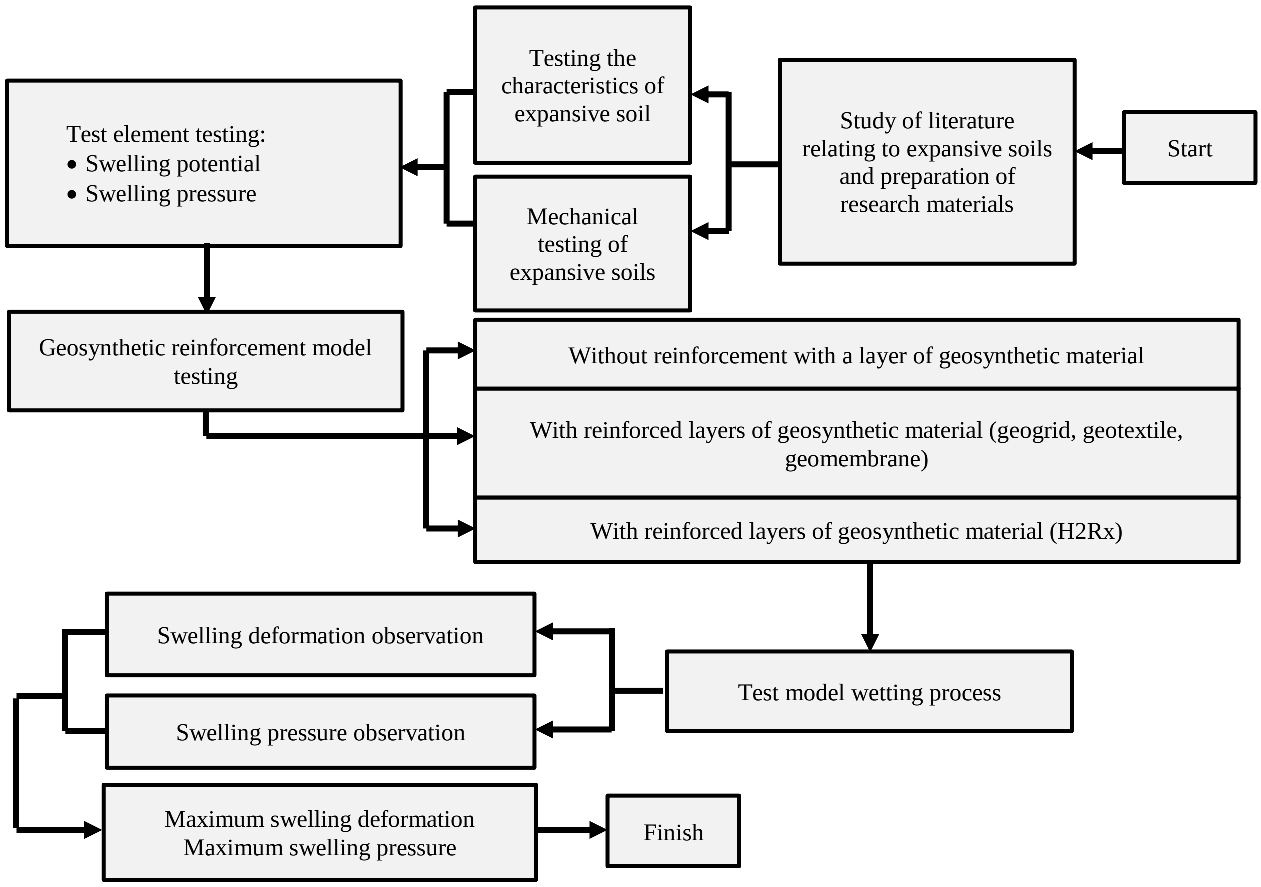


**Figure 3. Testing Process Flow**

Three test schemes were carried out: the test scheme without reinforcement, the test scheme with Geogrid, Geotextile, and Geomembrane reinforcement, and the test scheme with H2Rx reinforcement. The testing steps were carried out by inserting the soil into the testing tank with an adjusted thickness and giving it a layer of shaft as a water channel to speed up the process of expansive soil wetting. The total thickness of the expansion soil layer in the tank was 60 cm, which functions as a subgrade layer with a density according to the design of the CBR. After that, on top of the base soil layer, a lower foundation layer (subbase) was placed with granular soil material with a density by the design CBR. After the soil testing preparations have been completed, three swelling indicator sensors were installed to read the vertical deformation (swelling) and one indicator sensor to read the swelling pressure, which was placed in a predetermined position. The vertical deformation sensor was placed in the middle of the test model, and the second and third were put to the right and left of the test model, with a distance of 30 cm for each sensor from the center of the test model. The swelling pressure sensor was placed in the middle of the test model. The test model carried out can be seen in Figures 4a for the test model without reinforcement, 4b for the test with Geogrid, Geotextile, and Geomembrane reinforcement, and 4c for the test with H2Rx reinforcement.

To obtain good compaction by the planned design CBR value, the compaction was divided into three layers, each 30 cm thick. After that, compaction was carried out using the volume control method based on the dimensions that have been calculated. After compaction, the test sample was controlled for density value using the on-site soil density test method. This test was carried out to ensure that the density value for each test model has the same density value; this was very closely related to the swelling potential value and swelling pressure. Because the value of soil density dramatically affected the behavior of expansive soil.

The test model scheme also refers to the general specifications for road and bridge works. This test model was modeled as shown in Figure 4 to obtain data on swelling potential and swelling pressure. To analyze the reinforcement performance using a geosynthetic layer to control expansive soil behavior.

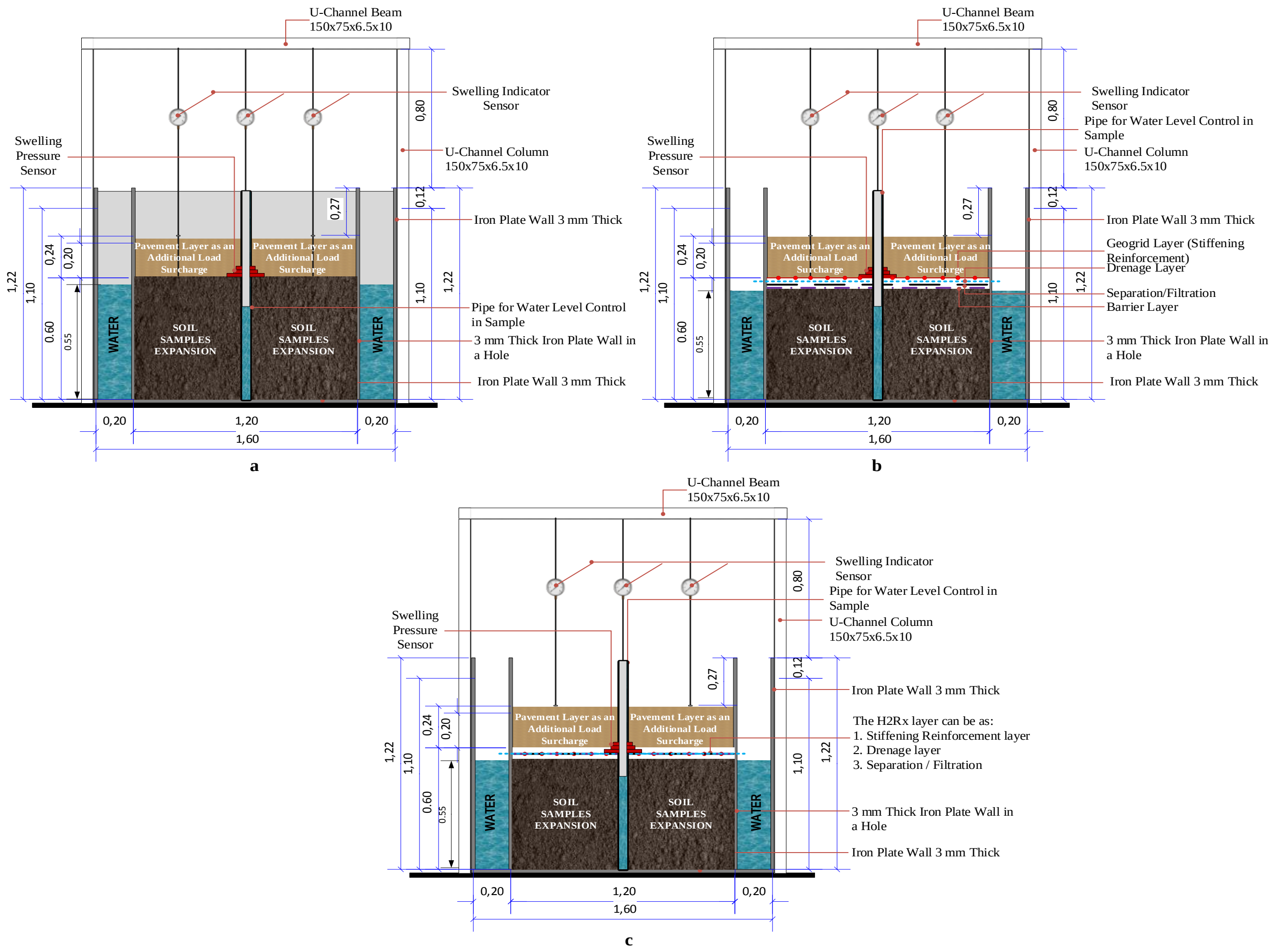


**Figure 4. Test Model Scheme: a. Model without Reinforcement; b. Geogrid, Geotextile, and Geomembrane Reinforcement Models; c. H2Rx Reinforcement Model**

The steps in the model testing process simulate water seeping into the soil, which can cause the soil to expand. This model can be seen in the testing scheme in Figure 5, where the testing process was modeled using a tub testing model filled with water on the right and left sides and expansive soil in the middle. The testing process was carried out by observing both visually and by recording vertical deformation and swelling pressure. The data recording process used a displacement sensor, modified into a deformation reading sensor and a swelling pressure sensor. Data recording was carried out every five seconds; the data was recorded and saved, and the recording was carried out during testing. The duration of the test was fifty-seven days; until there were no more extended changes in vertical deformation and soil pressure or the data obtained showed the same values or no more extended changes for three consecutive days, it was considered that the soil development process had been completed.


**Figure 5. Testing Model and Test Data Recording Process**

Measurements were carried out continuously for both vertical deformation and swelling pressure. The test results showed the relationship between the time water seeps into expansive soil, the deformation that caused expansion, and the swelling pressure when water seeps into the soil. From this test, the effect of the reinforcement carried out using geogrid, geotextile, and geomembrane layers, as well as reinforcement using the H2Rx layer, will be obtained and compared with that without reinforcement.

The results of this test will show the length of time of swelling, the amount of swelling that occurs, and the amount of swelling pressure that arises. The results of this test will be presented in the form of graphs that illustrate the relationship between time and swelling and the relationship between time and swelling pressure. It also presented the swelling pattern and the swelling pressure pattern that occurs. From this pattern, one can see the most significant swelling potential and the most considerable swelling pressure. As well as the performance effect of the geosynthetic reinforcement provided. During the test conditions, the instruments used for observation and the environmental conditions, namely controlled temperature and humidity, were controlled to minimize external influences.

# 3. Results and Discussion

## 3.1. Swelling Potential and Swelling Pressure Test Results

The results of the swelling deformation and swelling pressure tests using laboratory-scale testing on bonding tests using Geogrid, Geotextile, and Geomembrane can be seen in Figure 6, where the results of the swelling deformation are shown in Figure 6-a. This test showed that the sensor is placed in the middle (sensor 2), and the test model experienced the most considerable deformation of 63,662 mm. For sensors placed on the left and right (sensor one and sensor three), the test model experienced swelling deformation of 51.08 mm and 53.03 mm, respectively. A swelling pressure of 72.14 kPa can be seen in Figure 6-b.

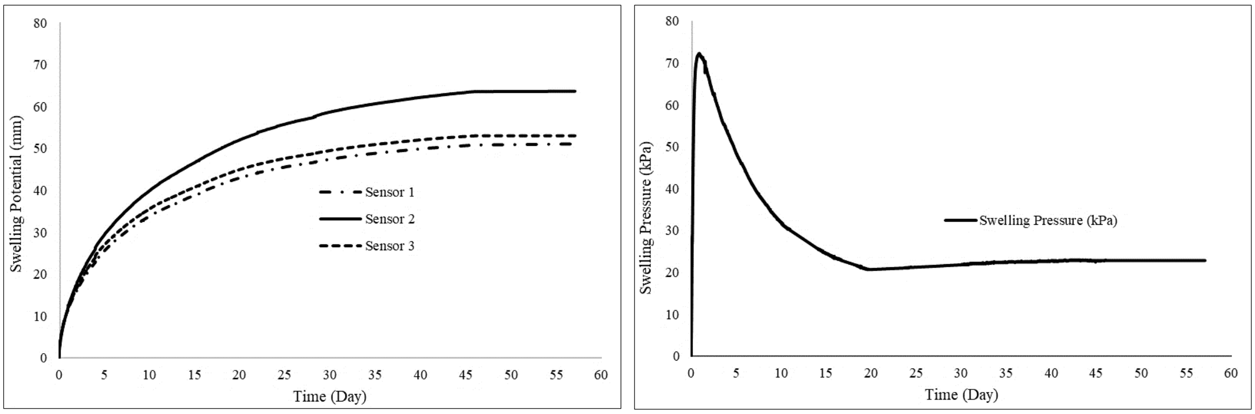


(a) (b)

**Figure 6. Swelling Potential and Swelling Pressure of Geogrid, Geotextile, and Geomembrane Reinforcement (a) Swelling Potential; (b) Swelling Pressure**

From the results of testing for swelling deformation and swelling pressure using laboratory scale testing on tests without reinforcement, results are obtained as in Figure 7, where the swelling deformation is seen in Figure 7-a; the test results showed that the placement of the sensor in the middle (sensor 2) of the test model experienced the maximum deformation of 103.31 mm. For sensors placed on the left and right (sensor one and sensor 3), the test model experienced swelling deformation of 90.14 mm and 84.33 mm, respectively—Figure 7-b results from a swelling pressure test of 423.93 kPa.

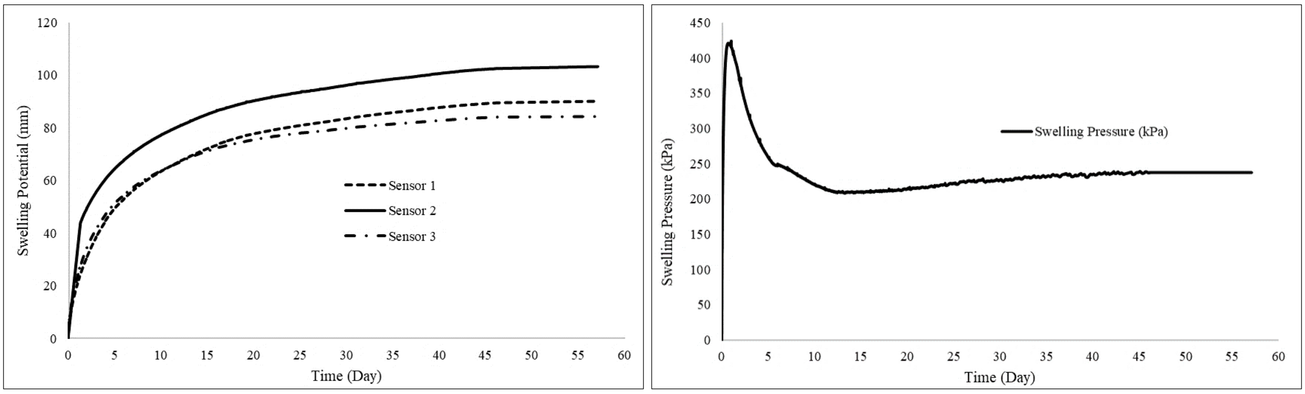


(a) (b)

**Figure 7. Swelling Potential and Swelling Pressure Without Reinforcement (a) swelling Potential; (b) swelling pressure**

In testing the swelling deformation and swelling pressure using a laboratory scale in the H2Rx reinforcement test, which is as seen in Figure 8, the maximum swelling deformation is seen in Figure 8a, where the test results show that the placement of the sensor in the middle (sensor 2) on the model deformation testing resulted in a maximum deformation of 68,782 mm. For sensors placed on the left and right (sensor 1 and sensor 3), the test model experienced swelling deformation of 60.98 mm and 58.66 mm, respectively. The swelling pressure test, shown in Figure 8b, is 132.86 kPa.

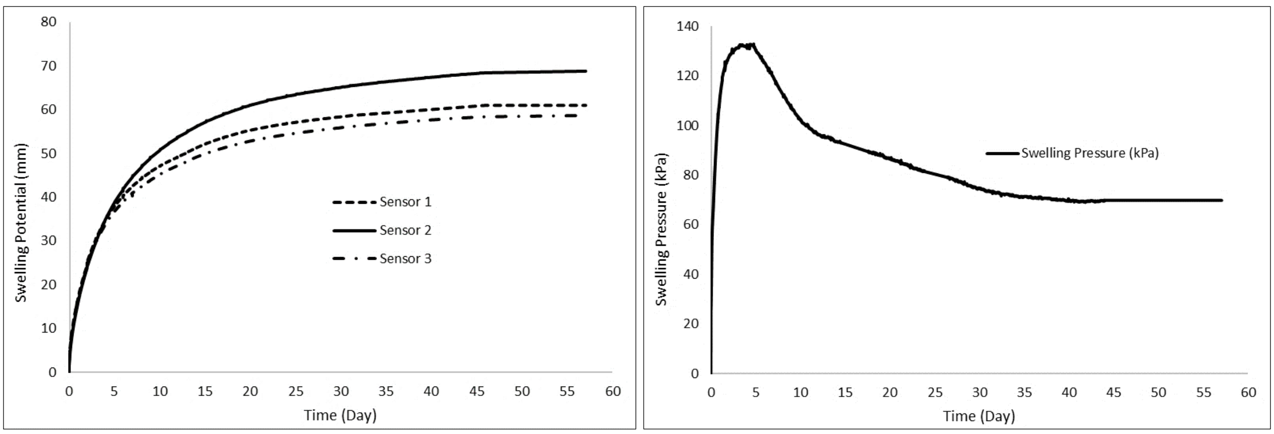


(a) (b)

**Figure 8. . Swelling Deformation and Swelling Pressure of H2Rx Reinforcement (a) Swelling Deformation; (b) Swelling Pressure**

Sensor readings placed in the middle experience the most significant deformation due to the stiffness effect of the testing tub, resulting in lateral direction swelling to the center of the testing tub. So that the most considerable deformation became centered in the middle, the placement of sensors on the left and right edges was not too deformed because the rigidity of the testing tub reduced the effect of lateral swelling. As for testing, the swelling pressure of the reinforcement used can reduce the expansive soil pressure because the swelling pressure was reduced evenly along the layer of reinforcement provided [4-7].

The test was stopped at a duration of 57 days because, from the results of observations, there was no longer a change in both development potential and development pressure that was significant and tended to be constant. For this test period, 57 days were conducted in the laboratory, and field testing was performed to confirm the laboratory test results with different soil types.

### 3.2. Swelling Potential

The effect of each reinforcement carried out in testing can be seen from the model testing results carried out on each test model scheme. The test results from sensor 1 can be explained in Figure 9, a comparison graph of swelling deformation, where for tests with Geogrid, Geotextile, and Geomembrane reinforcement, it was 51.08 mm; without reinforcement, it was 90.14 mm; and for H2Rx reinforcement, it was 60.98 mm. The results of this test showed that the size of the swelling at sensor 1 for the Geogrid, Geotextile, and Geomembrane layer reinforcement has the smallest value, and the H2Rx layer is slightly larger at 9.9 mm than the Geogrid, Geotextile, and Geomembrane reinforcement. The most considerable swelling occurs in the test model scheme without reinforcement.

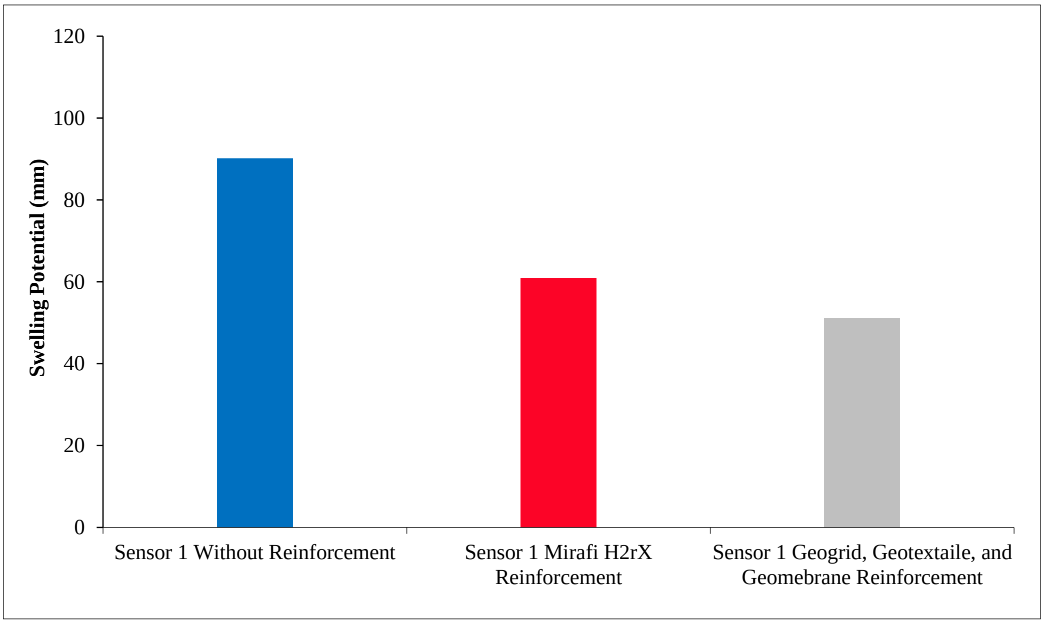


**Figure 9. Swelling Potential of Sensor 1**

For the test model carried out on each test model scheme, in Figure 10, the graph explains the comparison of swelling deformation on Sensor 2, where for testing without reinforcement, it was 103.31 mm; for H2Rx reinforcement, it was 68.78 mm; and with Geogrid, Geotextile, and Geomembrane reinforcement, it was 63.66 mm. The results of this test showed that the amount of swelling on sensor 2 for the Geogrid, Geotextile, and Geomembrane layer reinforcement had the smallest value, and the H2Rx layer was slightly larger at 5.12 mm than the Geogrid, Geotextile, and Geomembrane reinforcement. And the most significant swelling occurs in the scheme without reinforcement.

The comparison of test results for sensor 3 can be explained in Figure 11. The graph of the comparison of swelling deformation shows that for tests without reinforcement, it was 84.33 mm; with H2Rx reinforcement, it was 58.66 mm; and for reinforcement using Geogrid, Geotextile, and Geomembrane, it was 53.03 mm. The results of this test showed that the size of the swelling at sensor 3 for the reinforcement of the Geogrid, Geotextile, and Geomembrane layers has the smallest value, followed by the reinforcement of the H2Rx layer, which is slightly larger at 5.63 mm than the reinforcement of the Geogrid, Geotextile, and Geomembrane. The most considerable swelling occurs in the test model scheme without reinforcement.

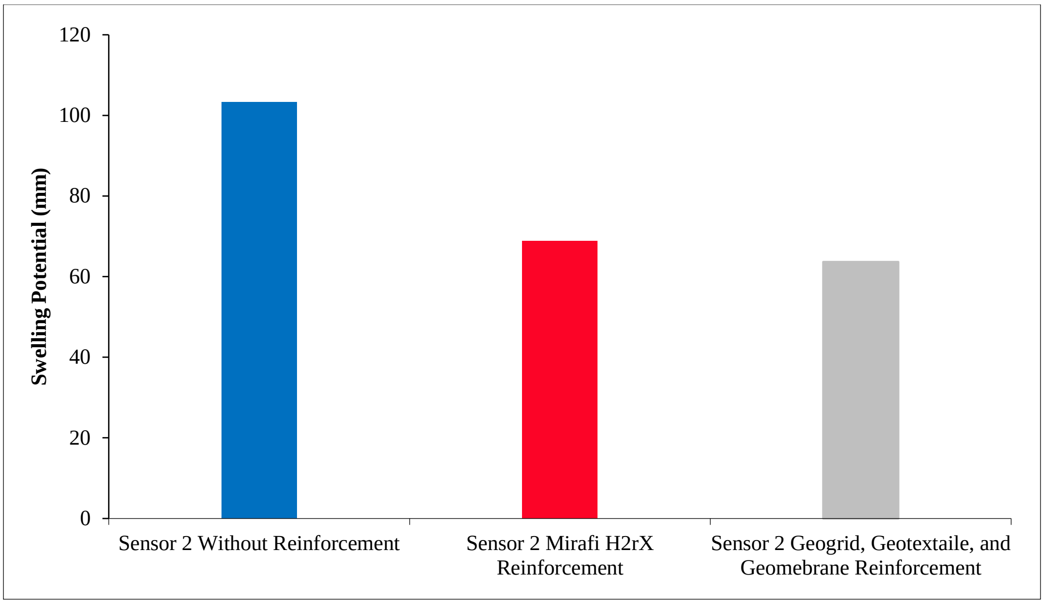


**Figure 10. Swelling Potential of Sensor 2**

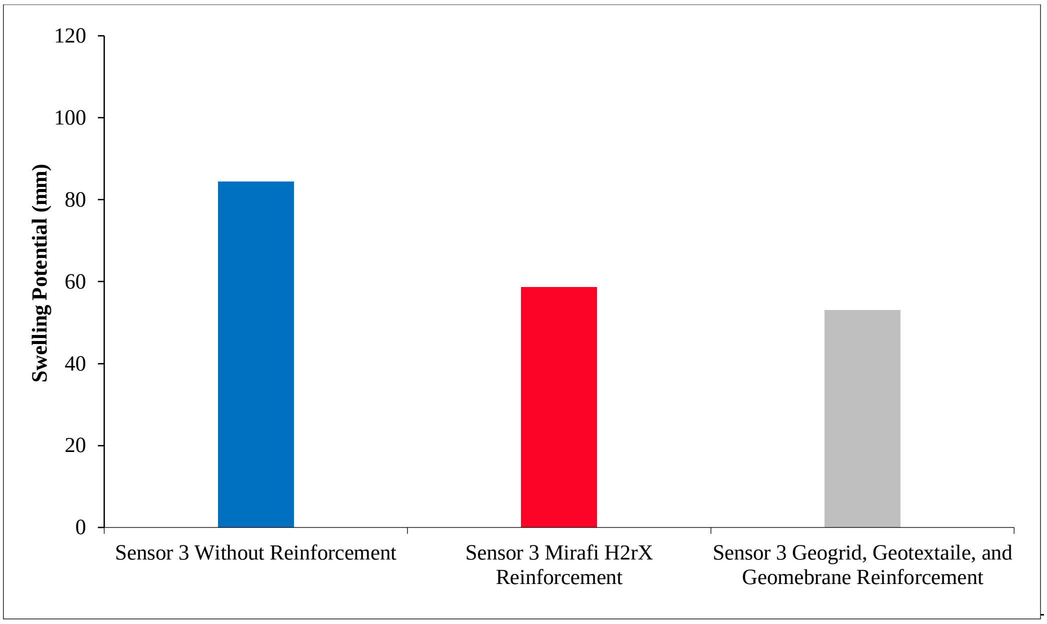


**Figure 11. Swelling Potential of Sensor 3**

From the test results for potential swelling, the presence of reinforcement using geogrid, geotextile, and geomembrane reinforcement layers or H2Rx reinforcement layers compared to no reinforcement can sufficiently reduce the potential swelling. The potential swelling can be well mobilized along the reinforcement layer provided. Because of the ability of both reinforcement layers, namely geogrid and H2Rx, each has good tensile strength to withstand the behavior of expansive soil swelling potential [2, 3].

### 3.3. Swelling Pressure

In the swelling pressure test on the test model scheme carried out, it can be seen that considerable swelling pressure occurs in each model that has been carried out. From the swelling pressure test, both without reinforcement using Geogrid, Geotextile, and Geomembrane reinforcement and reinforcement using H2Rx, it can be seen that the swelling pattern that occurs has the same pattern, where the most significant swelling pressure occurred when the water begins to seep into the soil. This can also be seen from the results of the unsoaked CBR test, which was compared with the CBR socket, which had experienced swelling, which resulted in a change in volume and the soil becoming soft so that the soil lost its bearing capacity. From the results of this test, the swelling pressure that occurs in the test model scheme without reinforcement is 423.93 kPa. For testing with H2Rx reinforcement, the swelling pressure that occurred was 132.86 kPa. As for development pressure testing with Geogrid, Geotextile, Geomembrane, and H2Rx reinforcement schemes, the results were 72.14 kPa, as shown in Figure 12.

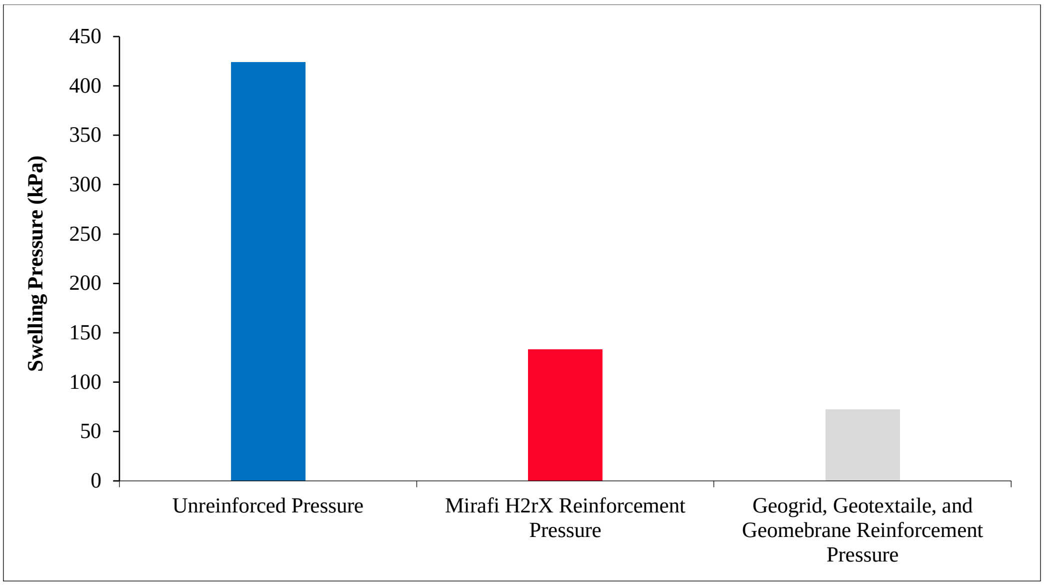


**Figure 12. Swelling Pressure Results**

For the results of the development pressure test, the reinforcement scheme made is very well able to reduce the development pressure. The geogrid, geotextile, and geomembrane reinforcement layers and the H2Rx reinforcement layer can mobilize and withstand the development pressure that occurs well. This happens because of the tensile strength of the geogrid and H2Rx reinforcement layers so that the development pressure is mobilized along the reinforcement layer, and the magnitude of the development pressure is well reduced by the tensile strength ability of the two reinforcement materials used in each test scheme [10].

### 3.4. Discussion

The results of tests on the behavior of expansive soil in terms of swelling potential showed that the reinforcement carried out using a geosynthetic layer greatly influences handling swelling deformations in expansive soil. The geosynthetic layer can adequately anticipate the swelling that occurs in expansive soil. The results of tests on the potential for swelling that occurs in expansive soil in each sensor reading show that the most significant amount of deformation occurs in the model scheme without reinforcement, which is a percentage of 100% compared to the model scheme with geosynthetic reinforcement.

In discussing the potential swelling that occurs, which can be seen in Figure 13, for strengthening the H2Rx layer at each sensor placement used, sensor 1 experienced swelling of 68%, sensor 2 of 67%, and sensor 3 of 70% of the potential swelling that occurred in the test scheme without reinforcement. For layers with geogrid, geotextile, and geomembrane reinforcement, for each sensor placement, the potential for swelling that occurs for sensor 1 was 57%. For sensor 2, it was 62%, and for sensor 3, it was 63% of the potential for swelling that occurred in the test scheme without reinforcement. The results of this test show that strengthening using H2Rx can reduce potential swelling by 32%, and strengthening geogrid, geotextile, and geomembrane can reduce potential swelling by 40%. These results show that the performance of geosynthetic reinforcement is very good at reducing the potential for swelling in expansive soil.

The results of testing the swelling potential using geogrid, geotextile, and geomembrane or H2Rx reinforcement layers were excellent in reducing and mobilizing the swelling potential as the function of these two pavement layers that had a tensile strength that can withstand the magnitude of potential swelling that occurred. However, H2Rx had the advantage of three tasks that simultaneously worked on one reinforcement material, which impacted the efficiency of work implementation and economics in financing. This was an advantage of the H2Rx reinforcement layer compared to the reinforcement layer using geogrid, geotextile, and geomembrane [34].

Strengthening carried out using a geosynthetic layer can significantly influence the amount of swelling pressure that occurs. The swelling pressure in the test scheme without reinforcement was the largest, at 100%. Meanwhile, for the test model scheme with H2Rx reinforcement, the swelling pressure that occurred was 31% of the scheme without reinforcement. For the reinforcement model scheme using geogrids, geotextiles, and geomembranes, the slightest swelling pressure occurs in 17% of the representation of the model scheme without reinforcement; this can be seen in Figure 14. In the swelling pressure test in each test scheme carried out on expansive soil behavior, the reinforcement using geosynthetics that was carried out dramatically influences the amount of swelling pressure that occurs [22, 35].

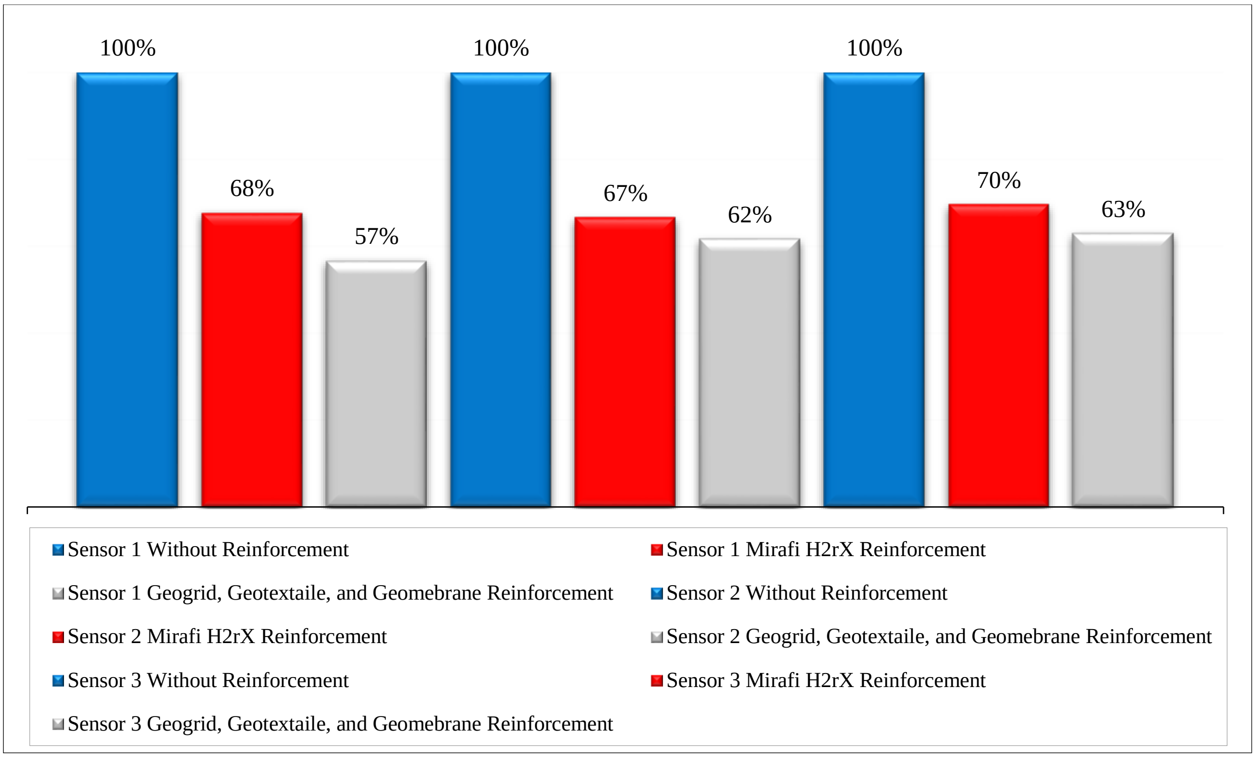


**Figure 13. Potential for Swelling**

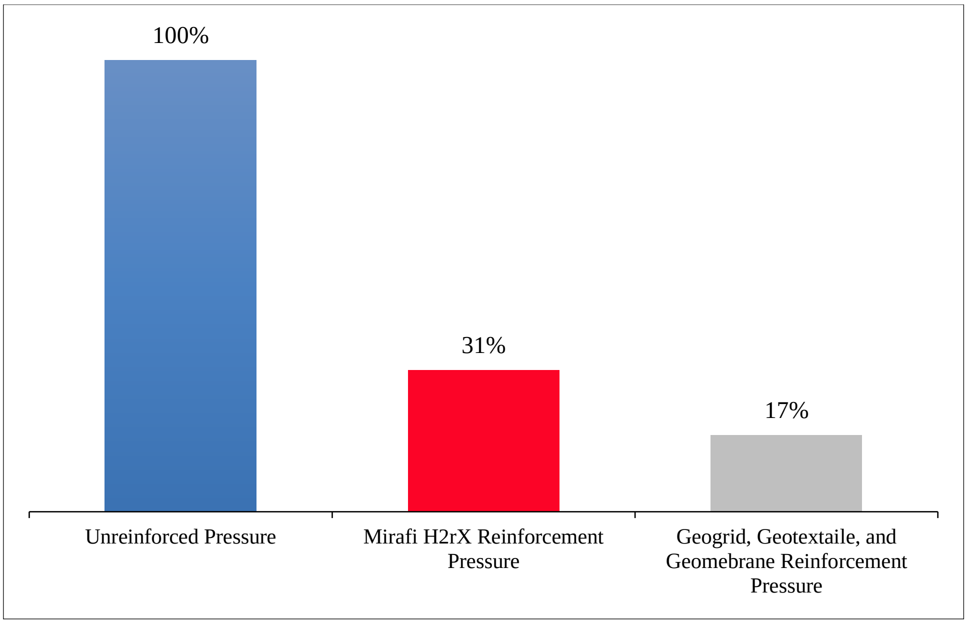


**Figure 14. Swelling Pressure**

Strengthening using a geosynthetic layer to overcome the swelling pressure in expansive soil shows promising results. The test results discussed show that reinforcement using H2Rx can reduce swelling pressure, which was represented by 69% of the swelling pressure that occurred in the test model scheme without reinforcement, and for geogrid, geotextile, and geomembrane reinforcement, it can reduce swelling pressure, which was represented by 83% of the test scheme without reinforcement. This demonstrates that geosynthetic reinforcement is highly effective at reducing swelling pressure in expansive soil.

The test results indicate that the geogrid, geotextile, geomembrane, and H2Rx reinforcement layers are highly effective at reducing and distributing swelling pressure due to their excellent tensile strength. The geogrid, geotextile, and geomembrane reinforcement layers are better than H2Rx from the test results. This is due to the materials' characteristics, especially the tensile strength of the two materials, a difference where the geogrid reinforcement layer has a tensile strength of 80 kN/m. In contrast, H2Rx has a tensile strength of 20 kN/m.

# 4. Conclusion

Using reinforcement with geosynthetic layers to overcome the behavior of expansive soils, both swelling potential and swelling pressure show test results that can reduce the behavior in expansive soils. The conclusion from the test results of the swelling potential shows that the reinforcement used, both by using H2Rx and geogrid, geotextile, and geomembrane, can reduce the swelling potential and make the swelling pressure smaller than without reinforcement in the test scheme. The results for reinforcement using H2Rx can reduce the potential swelling by 32%, which was represented against the test scheme without reinforcement. These results show that the reinforcement carried out on the test scheme using H2Rx can reduce the magnitude of the swelling pressure. This occurred because H2Rx can mobilize the potential swelling that arises along the layer and withstand the potential swelling that occurred. As well as for reinforcement, using geogrid, geotextile, and geomembrane layers can reduce the potential swelling by 40%, which was represented against the test scheme without reinforcement. This shows that the reinforcement scheme of geogrid, geotextile, and geomembrane layers can reduce the potential swelling that occurs in expansive soils and can mobilize the amount of potential swelling along the reinforcement layer so that the potential swelling that will occur because it is resistant to the geogrid, geotextile, and geomembrane reinforcement layers. From this test, the use of geosynthetic reinforcement materials, in this case, the H2Rx reinforcement layer, as well as the geogrid, geotextile, and geomembrane reinforcement layers, can be used as a reinforcement layer to reduce the potential for expansive soil swelling, especially in the pavement layer to avoid damage that occurs due to soil swelling that occurs.

In the swelling pressure test, geosynthetic reinforcement provides a perfect effect that can reduce the swelling pressure by more than 50% of the swelling pressure in the test model scheme without reinforcement. For reinforcement, using H2Rx can lessen the swelling pressure by 69%, representing against the swelling pressure without reinforcement. This is because H2Rx can reinforce and mobilize the pressure along the reinforcement layer in expansive soil when experiencing changes in water content. For reinforcement, using geogrid, geotextile, and geomembrane layers can reduce the swelling pressure by 83%, which is also represented against the swelling pressure without reinforcement. This also shows that geogrid, geotextile, and geomembrane reinforcement layers can mobilize the swelling pressure when expansive soil changes moisture content. Although from the test results conducted, reinforcement using layers of geogrid, geotextile, and geomembrane is better in terms of economy, efficiency, and effectiveness, it shows that reinforcement using H2Rx is more economical, efficient, and practical because it shows the results of the strength are not so different from the layers of geogrid, geotextile, and geomembrane. Currently, field testing is being carried out to prove the results of tests carried out in the laboratory and validate the test results in the laboratory, as well as observations that occur due to changing environmental conditions. The decrease in the development pressure on the reinforcement is due to the stress and development that arise well mobilized to both H2Rx and the Geogrid, Geotextile, and Geomembrane reinforcement layers.

# 5. Declarations

## 5.1. Author Contributions

Conceptualization, H. and T.H.; methodology, H.; software, H.; validation, T.H., A.R.D., and A.A.; formal analysis, H.; investigation, H.; resources, H.; data curation, H.; writing—original draft preparation, H.; writing—review and editing, H.; visualization, H.; supervision, T.H., A.R.D., and A.A., project administration, H.; funding acquisition, H. All authors have read and agreed to the published version of the manuscript.

## 5.2. Data Availability Statement

The data presented in this study are available on request from the corresponding author.

## 5.3. Funding

The authors received financial support from Indonesia Endowment Funds for Education (LPDP), Ministry of Finance of the Republic of Indonesia, for publishing this article.

## 5.4. Acknowledgments

The first author would like to thank the Lembaga Pengelola Dana Pendidikan (LPDP) of the Republic of Indonesia for providing financial support for the publication of this paper and also for the first author's doctoral study at Hasanuddin University, Indonesia, and also to SOLMAX Company for providing the geosynthetic materials used in this study.

## 5.5. Conflicts of Interest

The authors declare no conflict of interest.

## 6. References


[1] Bowles, J, E. (1986). Engineering Properties of Soils and Their Measurement. Singapore: McGraw-Hill, Inc, New York, United States.

[2] Teixeira, S. H. C., Bueno, B. S., & Zornberg, J. G. (2007). Pullout Resistance of Individual Longitudinal and Transverse Geogrid Ribs. Journal of Geotechnical and Geoenvironmental Engineering, 133(1), 37–50. doi:10.1061/(asce)1090-0241(2007)133:1(37).

[3] McCartney, J. S., Kuhn, J. A., & Zornberg, J. G. (2005). Geosynthetic drainage layers in contact with unsaturated soils. Proceedings of the 16th International Conference on Soil Mechanics and Geotechnical Engineering, 2301 - 2306. doi:10.3233/978-1-61499-656-9-2301.

[4] Li, C., & Zornberg, J. G. (2013). Mobilization of Reinforcement Forces in Fiber-Reinforced Soil. Journal of Geotechnical and Geoenvironmental Engineering, 139(1), 107–115. doi:10.1061/(asce)gt.1943-5606.0000745.

[5] Freilich, B. J., Li, C., & Zornberg, J. G. (2010). Effective shear strength of fiber-reinforced clays. 9th International Conference on Geosynthetics - Geosynthetics: Advanced Solutions for a Challenging World, ICG 2010, 23-27 May, 2010, Guarujá, Brazil.

[6] Zornberg, J. G. (2017). Functions and Applications of Geosynthetics in Roadways. Procedia Engineering, 189, 298–306. doi:10.1016/j.proeng.2017.05.048.

[7] Zornberg, J. G., & Gupta, R. (2009). Reinforcement of pavements over expansive clay subgrades. Proceedings of the 17th International Conference on Soil Mechanics and Geotechnical Engineering: The Academia and Practice of Geotechnical Engineering, 1, 765–768. doi:10.3233/978-1-60750-031-5-765.

[8] Liu, C.-N., Zornberg, J. G., Chen, T.-C., Ho, Y.-H., & Lin, B.-H. (2009). Behavior of Geogrid-Sand Interface in Direct Shear Mode. Journal of Geotechnical and Geoenvironmental Engineering, 135(12), 1863–1871. doi:10.1061/(asce)gt.1943-5606.0000150.

[9] Zornberg, J. G., & Gupta, R. (2010, May). Geosynthetics in pavements: North American contributions. Theme Speaker Lecture, Proceedings of the 9th International Conference on Geosynthetics, 23-27 May 2010, Guarujá, Brazil.

[10] Harianto, T. (2022). Performance of Subbase Layer with Geogrid Reinforcement and Zeolite-Waterglass Stabilization. Civil Engineering Journal (Iran), 8(2), 251–262. doi:10.28991/CEJ-2022-08-02-05.

[11] Zhang, R., Liu, Z., Zheng, J., & Zhang, J. (2020). Experimental Evaluation of Lateral Swelling Pressure of Expansive Soil Fill behind a Retaining Wall. Journal of Materials in Civil Engineering, 32(2), 04019360. doi:10.1061/(asce)mt.1943-5533.0003032.

[12] Zhang, R., Long, M., & Zheng, J. (2019). Comparison of Environmental Impacts of Two Alternative Stabilization Techniques on Expansive Soil Slopes. Advances in Civil Engineering, 9454929. doi:10.1155/2019/9454929.

[13] Dong, J. gui, Xu, G. yuan, Lv, H. bo, & Yang, J. yan. (2019). Prediction of Expansive Soil Strength Based on Micro-scale Properties. Geotechnical and Geological Engineering, 37(2), 869–882. doi:10.1007/s10706-018-0657-x.

[14] Xiao, J., Yang, H. P., Zhang, J. H., & Tang, X. Y. (2018). Surficial Failure of Expansive Soil Cutting Slope and Its Flexible Support Treatment Technology. Advances in Civil Engineering, 2018. doi:10.1155/2018/1609608.

[15] Liu, Y., & Vanapalli, S. K. (2017). Influence of Lateral Swelling Pressure on the Geotechnical Infrastructure in Expansive Soils. Journal of Geotechnical and Geoenvironmental Engineering, 143(6), 04017006. doi:10.1061/(asce)gt.1943-5606.0001651.

[16] Al-Omari, R. R. O., Fattah, M. Y., & Ali, H. A. (2016). Treatment of soil swelling using geogrid reinforced columns. Italian Journal of Geosciences, 135(1), 83–94. doi:10.3301/IJG.2014.54.

[17] Khan, M. S., Hossain, S., Ahmed, A., & Faysal, M. (2017). Investigation of a shallow slope failure on expansive clay in Texas. Engineering Geology, 219, 118–129. doi:10.1016/j.enggeo.2016.10.004.

[18] Liu, S., Lu, Y., Weng, L., & Bai, F. (2015). Field study of treatment for expansive soil/rock channel slope with soilbags. Geotextiles and Geomembranes, 43(4), 283–292. doi:10.1016/j.geotexmem.2015.04.004.

[19] Wang, L. J., Liu, S. H., & Zhou, B. (2015). Experimental study on the inclusion of soilbags in retaining walls constructed in expansive soils. Geotextiles and Geomembranes, 43(1), 89–96. doi:10.1016/j.geotexmem.2014.11.002.

[20] Hou, T. shun, Xu, G. li, Shen, Y. Jun, Wu, Z. Zhong, Zhang, N. Ning, & Wang, R. (2013). Formation mechanism and stability analysis of the Houba expansive soil landslide. Engineering Geology, 161, 34–43. doi:10.1016/j.enggeo.2013.04.010.

[21] Pathak, Y. P., & Alfaro, M. C. (2010). Wetting-drying behaviour of geogrid-reinforced clay under working load conditions. Geosynthetics International, 17(3), 144–156. doi:10.1680/gein.2010.17.3.144.

[22] Won, M.-S., & Kim, Y.-S. (2007). Internal deformation behavior of geosynthetic-reinforced soil walls. Geotextiles and Geomembranes, 25(1), 10–22. doi:10.1016/j.geotexmem.2006.10.001.

[23] Khoderagha, N., & Assaf, G. (2024). Assessment of Ground Penetrating Radar for Pyrite Swelling Detection in Soils. Civil Engineering Journal (Iran), 10(3), 729–737. doi:10.28991/CEJ-2024-010-03-05.

[24] ASTM C117-13. (2017). Standard Test Method for Materials Finer than 75-µm (No. 200) Sieve in Mineral Aggregates by Washing. ASTM International, Pennsylvania, United States. doi:10.1520/C0117-13.

[25] ASTM D7928-17. (2021). Standard Test Method for Particle-Size Distribution (Gradation) of Fine-Grained Soils Using the Sedimentation (Hydrometer) Analysis. ASTM International, Pennsylvania, United States. doi:10.1520/D7928-17.

[26] ASTM D4318-10. (2014). Standard Test Methods for Liquid Limit, Plastic Limit, and Plasticity Index of Soil. ASTM International, Pennsylvania, United States. doi:10.1520/D4318-10.

[27] ASTM D4943-08. (2018). Standard Test Method for Shrinkage Factors of Soils by the Wax Method (Withdrawn 2017). ASTM International, Pennsylvania, United States. doi:10.1520/D4943-08.

[28] AASHTO M 145-91. (2004). Classification of Soils and Soil-Aggregate Mixtures for Highway Construction purpose. American Association of State Highway and Transportation Officials (AASHTO), Washington, United States.

[29] ASTM D2487-17. (2020). Standard Practice for Classification of Soils for Engineering Purposes (Unified Soil Classification System). ASTM International, Pennsylvania, United States. doi:10.1520/D2487-17.

[30] ASTM D698-12. (2021). Standard Test Methods for Laboratory Compaction Characteristics of Soil Using Standard Effort (12,400 ft-lbf/ft$^3$ (600 kN-m/m$^3$)). ASTM International, Pennsylvania, United States. doi:10.1520/D0698-12R21.

[31] ASTM D1883-21. (2021). Standard Test Method for California Bearing Ratio (CBR) of Laboratory-Compacted Soils. ASTM International, Pennsylvania, United States. doi:10.1520/D1883-21.

[32] ASTM D2216-98. (2017). Standard Test Method for Laboratory Determination of Water (Moisture) Content of Soil and Rock by Mass. ASTM International, Pennsylvania, United States. doi:10.1520/D2216-98.

[33] ASTM D854-14. (2023). Standard Test Methods for Specific Gravity of Soil Solids by Water Pycnometer (Withdrawn 2023). ASTM International, Pennsylvania, United States. doi:10.1520/D0854-14.

[34] Basha, A., Azzam, W., & Elsiragy, M. (2024). Utilization of Sand Cushion for Stabilization of Peat Layer Considering Dynamic Response of Compaction. Civil Engineering Journal, 10(4), 1182–1195. doi:10.28991/CEJ-2024-010-04-011.

[35] Zhan, T. L. T., Chen, R., & Ng, C. W. W. (2014). Wetting-induced softening behavior of an unsaturated expansive clay. Landslides, 11(6), 1051–1061. doi:10.1007/s10346-013-0449-6.